ISSN 1061-933X, Colloid Journal, 2016, Vol. 78, No. 1, pp. 30–36. © Pleiades Publishing, Ltd., 2016.
Original Russian Text © P.N. Gevko, A.A. Zarubanov, K.S. Zhuravlev, L.G. Bulusheva, S.V. Larionov, A.V. Okotrub, 2016, published in Kolloidnyi Zhurnal, 2016, Vol. 78, No. 1, pp. 11–17.

The Influence of Water–Organic Solvent Composition on the Morphology and Luminescent Properties of CdS Nanoparticles Obtained by Chemical Precipitation

P. N. Gevko[a], A. A. Zarubanov[b], K. S. Zhuravlev[b, c], L. G. Bulusheva[a, c], S. V. Larionov[a, c], and A. V. Okotrub[a, c]

[a] *Nikolaev Institute of Inorganic Chemistry, Siberian Branch, Russian Academy of Sciences, pr. Akademika Lavrent'eva 3, Novosibirsk, 630090 Russia*

[b] *Institute of Semiconductor Physics, Siberian Branch, Russian Academy of Sciences, pr. Akademika Lavrent'eva 13, Novosibirsk, 630090 Russia*

[c] *Novosibirsk State University, ul. Pirogova 2, Novosibirsk, 630090 Russia*

e-mail: paul@niic.nsc.ru

Received May 19, 2015

Abstract—Cadmium sulfide (CdS) nanoparticles have been obtained by chemical precipitation onto the surface of single-crystalline silicon from an aqueous solution of ammonia, cadmium chloride ($CdCl_2$), and thiourea, as well as from water–DMSO and water–DMF mixtures with the same concentrations of the reagents. According to data of atomic force microscopy, the samples obtained from the aqueous solution consist of individual nanoparticles and agglomerates thereof with sizes of no larger than 1 μm. Materials obtained from the water–organic mixtures are distinguished by the aggregation of CdS nanoparticles into threadlike chains. The length of the formed curved chains and the size of CdS nanoparticles composing them depend on the nature and amount of an organic component of a mixture. Atomic force microscopy, transmission electron microscopy, and photoluminescence spectroscopy data have shown that the average size of CdS nanoparticles is 2–2.5 nm depending on solvent composition.

DOI: 10.1134/S1061933X16010075

INTRODUCTION

Optical, electronic, and catalytic properties of semiconductor nanoparticles differ significantly from those inherent in macroscopic bodies and depend on nanoparticle sizes [1–3]. The electronic properties of the nanoparticles may be regulated by varying their synthesis parameters and sizes. Nanoparticles of cadmium sulfide (CdS), which is a high-energy gap semiconductor with an energy gap width of the bulk material equal to 2.42 eV (at room temperature), are being extensively investigated. CdS is used in optical sensors, solar cells, light-emitting diodes, and other electrooptical devices. One of the problems relevant to the synthesis and extension of the fields of applications of semiconductor nanoparticles is the wide scatter in their sizes and the particle agglomeration during their synthesis, which leads to the loss of specific properties.

There are various methods for producing CdS nanocrystals with different shapes and sizes. For example, star-shaped CdS nanocrystals were obtained from a solution of a lyotropic triblock copolymer [4]. Nanosized CdS spheres were synthesized in water-in-oil microemulsions containing amphiphilic dendrimers [5]. Nanosized tetrahedrons, tetrapods, "needle-covered" balls, and hexagonal nanoprisms of CdS were prepared via the solvothermal synthesis using ethylenediamine/ethylene glycol mixed solvents [6]. CdS nanorods, nanowires, and nanotubes were synthesized in solutions by the hydrothermal method [7, 8]. When $Cd(NH_2C(S)NHNH_2)Cl_2$ complex is decomposed in a trioctylphosphine/trioctylphosphine oxide mixture, CdS nanorods with a diameter of 3–5 nm and a length of 10–24 nm are formed [9]. A simple one-stage method has been described in [10] for the preparation of long uniform CdS nanowires with a thickness of 1.7 nm from a solution of cadmium(II) hexadecylxanthate in hexadecylamine. CdS nanowires may also be obtained via electrochemical deposition [11].

Some methods have been proposed for suppressing coagulation of nanoparticles by introducing of thiols [12], phosphines [13], and amines [14] into solutions. Thus, the composition of a reaction mixture and synthesis parameters substantially affect the morphology of CdS nanoparticles.

One of the common methods for obtaining of metal sulfides, including CdS, in the form of fine particles and films is precipitation from aqueous solutions containing metal salts, sulfidizing agents, and ammonia or an alkali [15]. This relatively simple method is based on the use of low-toxic, objectionable-odor-free

sulfur-containing organic reagents, in particular, thiourea, $(NH_2)_2C=S$ (Thio), as sources of sulfur atoms [16–21]. It is interesting to study the synthesis of CdS from water–organic mixtures. The nature of a solvent and its donor ability are known to influence the stability of metal complexes [22–24]. The stability of Cd(II) complexes with Thio in mixed solvents increases with the concentration of an organic component [25, 26]. This increase may affect the chemical precipitation of CdS. In addition, solvation of CdS being formed by molecules of an organic solvent may influence the morphology of resulting CdS nanoparticles.

In this study, physicochemical properties of CdS nanoparticles obtained by chemical precipitation from water–dimethyl sulfoxide (DMSO) and water–dimethylformamide (DMF) mixed solvents onto silicon substrates have been investigated by atomic force microscopy (AFM), transmission electron microscopy (TEM), and photoluminescence (PL) spectroscopy. The influence of the nature and concentration of the organic solvent on the morphology of nanoparticles has been studied. The choice of these aprotic solvents has been dictated by their high, as compared with water, donor ability upon interaction with acceptors (donor numbers DN_{SbCl5} are 18.0, 26.6, and 29.8 for H_2O, DMF, and DMSO, respectively [22]), as well as their low toxicity and volatility. Solvation of the surface of primary CdS particles with DMSO and DMF molecules via C=O and S=O groups may lead to stabilization of particles owing to the shielding role of methyl groups [27, 28].

EXPERIMENTAL

CdS nanoparticles were prepared by chemical precipitation from an aqueous solution (200 mL) of ammonia (70.3 g/L) containing$CdCl_2$ (0.015 mol/L) and Thio (0.15 mol/L) according to the procedure described in [29, 30], as well as from H_2O–DMSO and H_2O–DMF mixtures with the same concentrations of NH_3, $CdCl_2$, and Thio. The mixed solvents contained different amounts of DMSO or DMF. The synthesis was carried out in an open beaker heated in a water bath at 40°C for 10 min. Such a short time of a silicon substrate exposure in a solution was chosen in order to avoid deposition of nanoparticles formed in a solvent onto the substrate. Nanoparticles were formed on the surface (100) of single-crystalline silicon substrates immersed in a solution with the help of a holder. Several samples were obtained from the aqueous solution (H_2O-100) and mixed water–organic solvents containing 50 vol % of DMF (DMF-50) or DMSO (DMSO-50) and 20 vol % of DMF (DMF-20) or DMSO (DMSO-20).

The morphology of CdS nanoparticles was investigated using a SolverPro atomic force microscope (NT-MDT, Russia) and a JEOL 2010 transmission electron microscope. In the AFM experiments, surface areas with sizes of 3×3 μm^2 (±10%) were scanned with NSG01 DLC (NT-MDT) supersharp tips having a curvature radius smaller then 1 nm and an average value of the nominal spring constant of 5.5 N/m. The measurements were performed in a tapping mode. Samples for TEM examinations were subjected to ultrasonic dispersing, and CdS particles were transferred onto a grid substrate at the onset of the cavitation boiling of a suspension.

A stationary PL was excited with a continuous He–Cd laser operating at a wavelength of 325 nm and a radiation power of about 0.5 W/cm^2. The PL spectra were recorded with a spectrometer designed on the basis of an SDL-1 double monochromator equipped with a cooled FEU-79 photomultiplier operating in a single photon counting mode.

RESULTS AND DISCUSSION

Morphologcal Studies of Nanoparticles

AFM images of samples containing CdS nanoparticles located on the Si(100) surface are shown in Fig. 1. It can be seen that the samples obtained from mixed water–organic solvents consist mainly of nanoparticles and threadlike agglomerates thereof. The largest amount of relatively coarse individual CdS particles is seen in the image of the H_2O-100 sample (Fig. 1a). Smaller nanoparticles form nanothreads. Previously, the same picture was observed when studying CdS particles on silicon substrates by scanning electron microscopy [29]. It was noted that, at an initial stage of the process, CdS nanoparticles with gradually increasing sizes were formed on the silicon surface. The diameter of the threadlike structures remained almost unchanged, while their number increased up to the formation of networks of nanothreads on the substrate. Thus, our data are consistent with previously reported results.

The synthesis of monodisperse CdS nanoparticles, rods, and rodlike structures has mainly been described in the literature. The formation of chain structures from individual almost spherical nanoparticles (aspect ratio ≈1) is clearly observed in the AFM image taken in the phase contrast mode (Fig. 1f), where narrow areas of the contact between adjacent particles may be distinguished.

In contrast to nanorods, nanothreads have a considerable amount of bends indicating the absence of a long-range crystalline order. The length and diameter of the nanothreads vary from sample to sample depending on the nature and amount of an organic component in a water–organic mixture. Henceforward, the term "average size of nanoparticles" will mean the averaged value the of profile height of both individual nanoparticles and nanothreads on a substrate, because they are approximately equal. The average size of nanoparticles in the threads of the H_2O-100 sample as determined by AFM is about 2.5

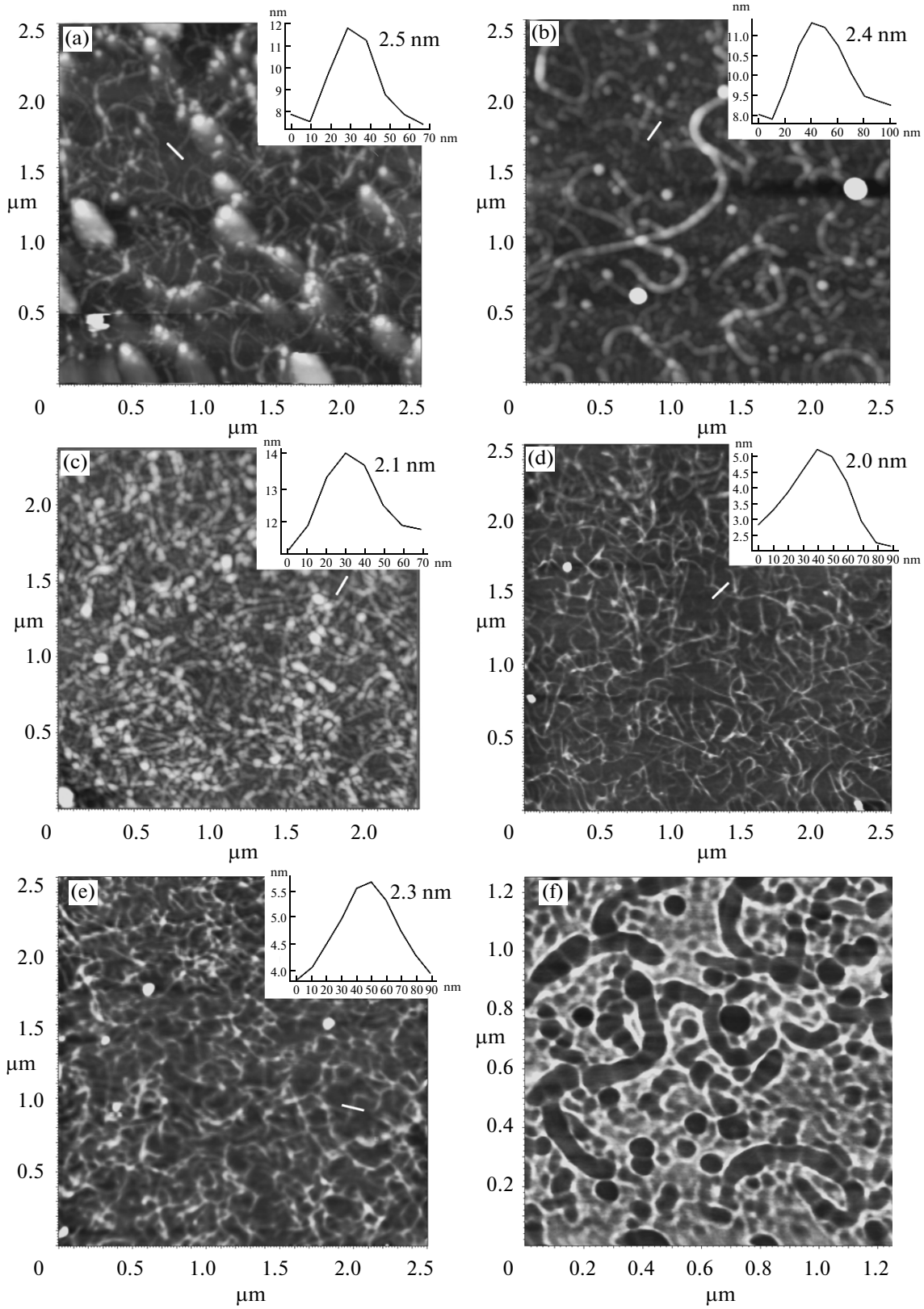

Fig. 1. AFM images of CdS nanoparticles for (a) H_2O-100, (b) DMF-50, (c) DMF-20, (d) DMSO-50, and (e) DMSO-20 samples. (f) Image obtained by phase mapping for chains in DMF-50 sample; it can be seen that nanothreads consist of individual segments separated by thinner necks. The insets present the profiles and heights of nanoparticles; the sections are drawn in the places denoted in the figures.

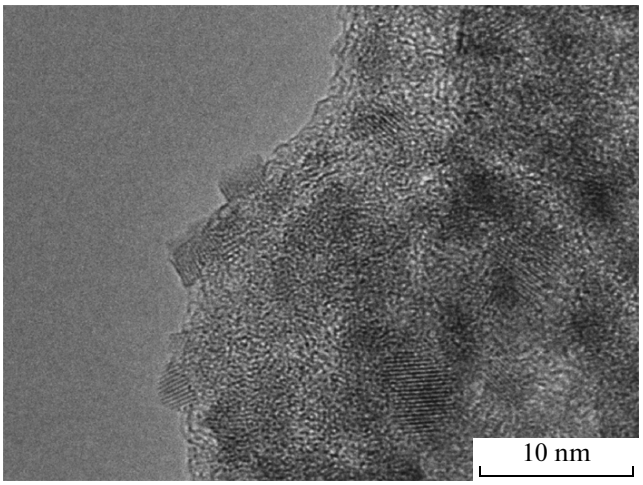

Fig. 2. TEM image of CdS nanoparticles synthesized in mixed water–organic solution (DMF-50 sample).

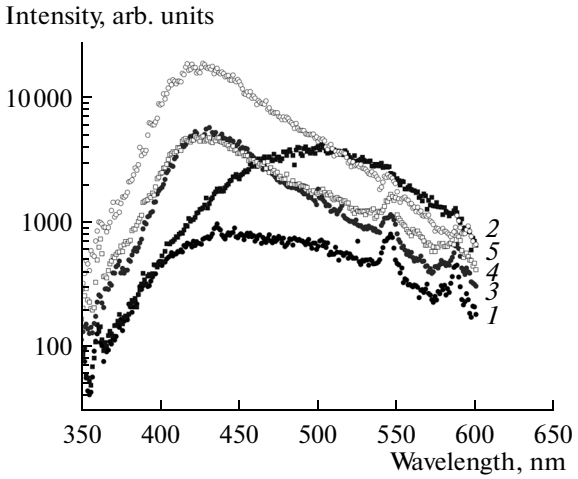

Fig. 3. PL spectra recorded at 77 K for CdS nanoparticles of (*1*) H_2O-100, (2) DMF-50, (*3*) DMSO-50, (*4*) DMF-20, and (*5*) DMSO-20 samples.

nm, which agrees with the data presented in [31]. In the DMF-50 sample (Fig. 1b), individual CdS particles and nanothreads with a diameter of ≈2.9 nm are observed. In the DMF-20 sample, the fraction of individual nanoparticles is considerably smaller, and the chains are shorter than those in the H_2O-100 and DMF-50 samples; however, their number is increased (Fig. 1c). The average size of nanoparticles is ≈2.1 nm. When DMSO is used as an organic solvent in the synthesis, individual CdS nanoparticles are almost absent, and nanothreads alone are observed. The average size of the particles in DMSO-50 is ≈2.3 nm (Fig. 1d), and that in the DMSO-20 sample has decreased to ≈2.0 nm (Fig. 1e). The data obtained show the influence of medium composition on the morphology of the particles: a decrease in the content of the organic component of the water–organic mixtures has led to some reduction in the sizes of CdS nanoparticles. It is interesting that the smallest particles are observed in the DMF-20 and DMSO-20 samples. Moreover, the use of H_2O–DMSO mixtures has led to the predominant formation of nanothreads from CdS nanoparticles.

Figure 2 depicts the TEM image of nanoparticles in the DMF-50 sample. The ultrasonic treatment of the sample has resulted in the disintegration of the nanothreads into individual CdS particles. However, the average size of the particles is, according to the TEM data, close to the values obtained by AFM and is about 3 nm.

Photoluminescent Properties of CdS Nanoparticles

Photoluminescence (PL) spectra of the samples measured at 77 K are shown in Fig. 3. A high-energy peak with a maximum at about 420 nm (2.95 eV) dominates in the spectra of the DMSO-50, DMF-20, and DMSO-20 samples. The PL spectra of the H_2O-100 and DMF-50 samples comprise a broad band, which seems to be a superposition of at least two bands. The high-energy peaks correspond to energy higher than the energy gap width of bulk CdS (2.58 eV) [31]. We believe that the high-energy peak is due to the electron transitions between size quantization levels in CdS nanoparticles. Luminescence in a wavelength range of 490–500 nm seems to be due to the "zone–zone" recombination in large particles, in which the size quantization effect is absent. The PL intensities of all studied samples are reduced by more than an order of magnitude at 300 K. This is probably due to the thermal activation of nonradiative recombination channel. In the DMSO-20 sample, radiation of large particles prevails.

PL spectra were approximated by the example of the DMSO-50 sample. The spectrum is adequately described by a superposition of two Gaussian curves (Fig. 4) with maxima at wavelengths of 420 and 490 nm, which correspond to energies of 2.95 and 2.53 eV, respectively. The first maximum is associated with an optical transition between size quantization levels of a CdS nanoparticle; the energy of 2.53 eV is in good agreement with the energy gap width of bulk CdS having the hexagonal lattice (2.58 eV at 0 K) [31].

DMSO or DMF content in mixed solvents influences the position of the maximum and the width at the half-height of a PL peak (Fig. 3). When DMF content in the mixture is increased to 50%, the PL maximum shifts toward lower energies, while, when DMSO content in the water–organic mixture is elevated, the position of the maximum remains almost unchanged. On the other hand, an increase in the DMSO or DMF content in the mixture leads to a decrease in the peak width at the half-height. However, the peak width at the half-height is 10% smaller for nanoparticles obtained in the H_2O–DMSO mix-

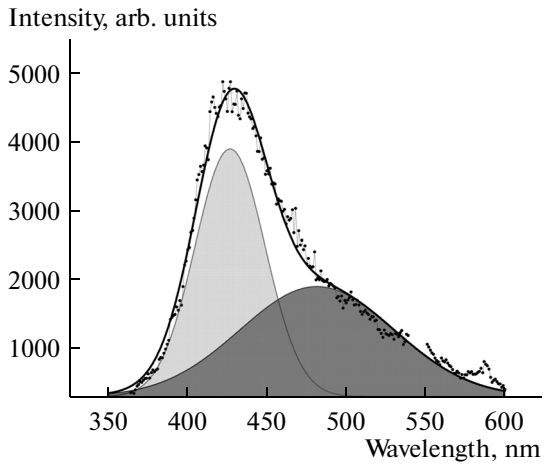

Fig. 4. PL spectrum of DMSO-50 sample nanoparticles and its approximation by two Gaussian components.

ture than that for nanoparticles synthesized in the H_2O–DMF mixture.

Nanocrystal size distribution may be determined from PL spectra using a model quantum well with infinitely high walls. In this case, radiation energy is uniquely related to the minimal size of nanoparticles:

$$E = E_{g0} + \frac{\hbar^2 n^2}{2m^* d^2},$$

where E is the energy between size quantization levels of an electron and a hole (radiation energy), E_{g0} is the energy gap width of a bulk material, $\hbar$ is the Planck constant, n is a positive integer, $m^* = m_e m_h/(m_e + m_h) = 0.154m_0$ is the reduced effective mass of an electron and a hole ($m_e = 0.19m_0$ and $m_h = 0.8m_0$ are effective masses of the electron and the hole, respectively), m_0 is the mass of a free electron, and d is nanoparticle size. The nanocrystal size distribution of the DMSO-50 sample is exemplified in Fig. 5. While plotting the diagram, we assumed that the particle size may be found from the radiation energy, whereas the PL intensity is directly proportional to the number of nanoparticles. CdS particles larger than 6 nm may be considered as a bulk material. This approach is rather rough, but it enables one to estimate the sizes of nanoparticles corresponding to the maximum of the distribution.

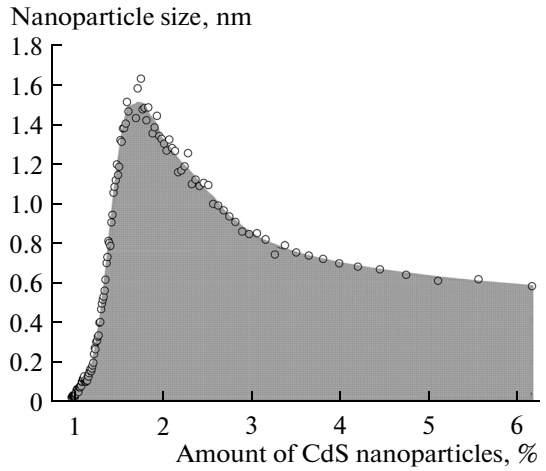

Fig. 5. Size distribution of CdS nanoparticles in DMSO-50 sample plotted from PL spectroscopy data.

Dependences of nanoparticle size on the percentage of an organic component in a solution plotted from the AFM and PL spectroscopy data are shown in Fig. 6. It can be seen that, in the H_2O–DMF mixture, CdS nanoparticles are slightly larger than those in the H_2O–DMSO solvent. In addition, an increase in the content of the organic component in the mixed solvent to 50% leads to a growth in the size of nanoparticles. Thus, the change in the size of CdS nanoparticles depending on the content and the type of an aprotic donor solvent in a water–organic mixture revealed by the analysis of AFM images of the samples is confirmed by the data of PL spectroscopy.

The Influence of Solvent Composition on the Morphology and Sizes of CdS Nanoparticles

Previously, the study of the mechanism of CdS formation in an aqueous solution containing $CdCl_2$, Thio, and ammonia indicated the formation of mixed-ligand Cd(II) complexes containing NH_3 molecules and a Thio molecule coordinated with the Cd^{2+} ion via the S atom [15, 32]. Then, the alkaline hydrolysis of Thio molecules occurs, which leads to the rupture the bond between carbon and sulfur atoms and the formation of paired units of CdS. In the opinion of the

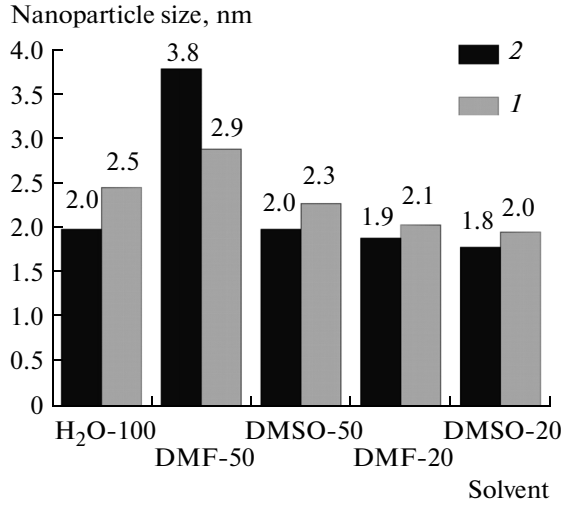

Fig. 6. Average sizes of CdS nanoparticles in H_2O-100, DMF-50, DMSO-50, DMF-20, and DMSO-20 samples according to (*1*) AFM and (*2*) PL spectroscopy data.

authors of [15], CdS pairs form primary $(CdS)_n$ clusters in the solution; then, the primary particles are aggregated via the contacts between them.

The formation mechanism of CdS subunits is the same in the aqueous solution and mixed solvents. At the same time, DMF and DMSO change the interaction of primary CdS nanoparticles with each other as compared with the aqueous solution. Nanoparticles formed during the initial minutes of the synthesis may have a surface charge and a dipole moment. The molecules of strong donor solvents (DMF and DMSO) are adsorbed on the surface of the acceptors (CdS nanoparticles), thereby promoting the stabilization of the particles and preventing them from aggregation; however, CdS nanoparticles exhibit a tendency to the formation of chainlike associates. The formation of the chains may be explained by the tendency of the nanoparticles to association in the (0001) direction, which corresponds to the most active crystallographically oriented sites of the surface of hexagonal CdS nanoparticles [34]. The extent of the influence of DMSO and DMF on the formation of isolated CdS nanoparticles and chainlike structures is obviously determined by their ability to solvate the particles. The employed solvents create more extended and anisotropic solvation shells on them than does water. The strength of the solvation shell depends on a number of factors, including donor number DN_{SbCl_5} of a solvent, the size of a solvent molecule, and the concentration of an organic solvent in a solution. Since DMSO has a high donor number DN_{SbCl_5}, the strongest solvation shell is formed in an H_2O–DMSO mixture, thus leading to more efficient stabilization of CdS nanoparticles than that upon synthesis in the aqueous solution and a H_2O–DMF mixture at the same ratio of the mixed solvent components. Some increase in the size of CdS nanoparticles obtained in the mixed solvent containing 50% DMF is probably due to the fact that this mixture has a lower dielectric permittivity than do the other studied mixtures and water (for H_2O, DMSO, and DMF, it is equal to 81.0, 45.0, and 36.1, respectively) [22]. This may well lead to the formation of largest $(CdS)_n$ clusters in this mixture. The data obtained will be useful for the development of studies in the field of chemistry of semiconductor nanoparticles [34].

CONCLUSIONS

The structure and optical properties of CdS nanoparticles obtained in aqueous solutions of NH_3, $CdCl_2$, and Thio and in mixed solvents, in which 20 or 50 vol % of water has been replaced by DMSO or DMF, and precipitated onto the surface of a silicon substrate have been investigated by AFM, TEM, and PL spectroscopy. It has been shown that CdS nanoparticles may form chains, the sizes of which depend on solvent composition. Analysis of the PL spectra has shown that, along with nanocrystals having average sizes of 1.8–3.8 nm, the obtained samples contain larger nanoparticles with the optical transition energy corresponding to the energy gap width of a bulk hexagonal CdS crystal. It has been assumed that the influence of DMSO and DMF on the formation of CdS nanoparticles and chainlike structures is determined by the solvation properties of solvent molecules, as well as the value of the dielectric permittivity of a mixed water–organic solvent.

ACKNOWLEDGMENTS

We are grateful to A.V. Ishchenko for supplying TEM images.

REFERENCES

1. Tret'yakov, Yu.D., *Vestn. Ross. Akad. Nauk*, 2010, vol. 80, p. 591.
2. Gubin, S.P., Kataeva, N.A., and Khomutov, G.B., *Izv. Ross. Akad. Nauk, Ser. Khim.*, 2005, p. 811.
3. Rempel', A.A., *Izv. Ross. Akad. Nauk, Ser. Khim.*, 2013, p. 857.
4. Chae, W.-S., Shin, H.-W., Lee, E.-S., Shin, E.-J., Jung, J.-S., and Kim, Y.-R., *J. Phys. Chem. B*, 2005, vol. 109, p. 6204.
5. Wang, F., Xu, G., Zhang, Z., and Xin, X., *Eur. J. Inorg. Chem.*, 2006, p. 109.
6. Chu, H., Li, X., Chen, G., Zhou, W., Zhang, Y., Jin, Z., Xu, J., and Li, Y., *Cryst. Growth Des.*, 2005, vol. 5, p. 1801.
7. Yang, J., Zeng, J.-H., Yu, S.-H., Yang, L., Zhou, G.-E., and Qian, Y.-T., *Chem. Mater.*, 2000, vol. 12, p. 3259.
8. Tang, K.-B., Qian, Y.-T., Zeng, J.-H., and Yang, X.-G., *Adv. Mater.* (Weinheim, Fed. Repub. Ger.), 2003, vol. 15, p. 448.
9. Nair, P.S., Radhakrishnan, T., Revaprasadu, N., Kolawole, G.A., and O'Brien, P., *Chem. Commun.*, 2002, p. 564.
10. Xiong, Y., Xie, Y., Yang, J., Zhang, R., Wu, C., and Du, G., *J. Mater. Chem.*, 2001, vol. 12, p. 3712.
11. Xu, D., Xu, Y., Chen, D., Guo, L., Gui, L., and Tang, Y., *Adv. Mater.* (Weinheim, Fed. Repub. Ger.), 2000, vol. 12, p. 520.
12. Xu, D., Liu, Z., Liang, J., and Qian, Y., *J. Phys. Chem. B*, 2005, vol. 109, p. 14344.
13. Acharya, S., Patla, I., Kost, J., Efrima, S., and Golan, Y., *J. Am. Chem. Soc.*, 2006, vol. 128, p. 9294.
14. Yang, Y., Chen, H., Mei, Y., Chen, J., Wu, X., and Bao, X., *Solid State Commun.*, 2002, vol. 123, p. 279.
15. Markov, V.F., Maskaeva, L.N., and Ivanov, P.N., *Gidrokhimicheskoe osazhdenie plenok sul'fidov metallov* (Hydrochemical Deposition of Metal Sulfide Films), Yekaterinburg: Uralsk. Otd., Ross. Akad. Nauk, 2006.
16. Kitaev, G.A., Uritskaya, A.A., and Mokrushin, S.G., *Zh. Fiz. Khim.,* 1965, vol. 39, p. 2065.
17. Kitaev, G.A. and Uritskaya, A.A., *Izv. Akad. Nauk SSSR, Ser. Neorg. Mater.*, 1966, vol. 2, p. 1554.
18. Leonova, T.G., Kramareva, T.G., and Shul'man, V.M., *Kolloidn. Zh.*, 1968, vol. 30, p. 61.

19. Bogdanovich, V.B., Velikanov, A.A., Kaganovich, E.B., Ostrovskaya, I.K., and Svechnikov, S.V., *Neorg. Mater.*, 1971, vol. 7, p. 2075.
20. Semenov, V.N., Averbakh, E.M., and Mikhaleva, L.I., *Zh. Neorg. Khim.*, 1979, vol. 24, p. 911.
21. Markov, V.F. and Maskaeva, L.N., *Izv. Ross. Akad. Nauk, Ser. Khim.*, 2014, p. 1523.
22. Gutmann, V., *Coordination Chemistry in Nonaqueous Solutions*, Vienna: Springer, 1968.
23. Krestov, G.A., Afanas'ev, V.N., Agafonov, A.V., and Shormanov, V.A., *Kompleksoobrazovanie v nevodnykh rastvorakh* (Complexation in Nonaqueous Solutions), Moscow: Nauka, 1989.
24. Burger, K., *Experimental Methods for Investigation of Solvation, Ionic and Complex Formation Reactions in Nonaqé*miai Kiadó, 1982.
25. Lavrenova, L.G., Larionov, S.V., and Zegzhda, T.V., *Izv. Akad. Nauk SSSR, Ser. Khim.*, 1974, no. 5, p. 63.
26. Tulyupa, F.M., Baibarova, E.Ya., Movchan, V.V., and Dzyuba, O.G., *Zh. Neorg. Khim.*, 1979, vol. 24, p. 389.
27. Lotfi Orimi, R., Shahtahmasebi, N., Tajabor, N., and Kompany, A., *Phys. E* (Amsterdam), 2008, vol. 40, p. 2894.
28. Yu, Z., Qu, F., and Wu, X., *Dalton Trans.*, 2014, vol. 43, p. 4847.
29. Kudashov, A.G., Leonova, T.G., Kurenya, A.G., Danilovich, V.S., Bulusheva, L.G., Larionov, S.V., and Okotrub, A.V., *Izv. Ross. Akad. Nauk, Ser. Khim.*, 2010, p. 1674.
30. Okotrub, A.V., Asanov, I.P., Larionov, S.V., Kudashov, A.G., Leonova, T.G., and Bulusheva, L.G., *Phys. Chem. Chem. Phys.*, 2010, vol. 12, p. 10871.
31. Brus, L.E., *J. Chem. Phys.*, 1984, vol. 80, p. 44039.
32. Leonova, T.G. and Kazbanov, V.I., *Izv. Sib. Otd. Akad. Nauk SSSR, Ser. Khim.*, 1977, no. 3, p. 108.
33. Son, J.S., Park, K., Kwon, S.G., Yang, J., Choi, M.K., Kim, J., Yu, J.H., Joo, J., and Hyeon, T., *Small*, 2012, vol. 8, p. 2394.
34. Kozhevnikova, N.S., Vorokh, A.S., and Uritskaya, A.A., *Usp. Khim.*, 2015, vol. 84, p. 225.

Translated by V. Kudrinskaya